Deficiency in cytosine DNA methylation leads to high chaperonin expression and tolerance to aminoglycosides in Vibrio cholerae

André Carvalho, Didier Mazel, Zeynep Baharoglu

Deficiency in cytosine DNA methylation leads to high chaperonin expression and tolerance to aminoglycosides in *Vibrio cholerae*

André Carvalho[1,2], Didier Mazel[1]*, Zeynep Baharoglu[1]*

[1] Département Génomes et Génétique, Institut Pasteur, UMR3525, CNRS, Unité Plasticité du Génome Bactérien, Paris, France

[2] Sorbonne Université, Collège doctoral, F-75005 Paris, France

* corresponding authors, mazel@pasteur.fr, zeynep.baharoglu@pasteur.fr

ABSTRACT

Antibiotic resistance has become a major global issue. Understanding the molecular mechanisms underlying microbial adaptation to antibiotics is of keen importance to fight Antimicrobial Resistance (AMR). Aminoglycosides are a class of antibiotics that target the small subunit of the bacterial ribosome, disrupting translational fidelity and increasing the levels of misfolded proteins in the cell. In this work, we investigated the role of VchM, a DNA methyltransferase, in the response of the human pathogen *Vibrio cholerae* to aminoglycosides. VchM is a *V. cholerae* specific orphan m5C DNA methyltransferase that generates cytosine methylation at 5'-R**C**CGGY-3' motifs. We show that deletion of *vchM,* although causing a growth defect in absence of stress, allows *V. cholerae* cells to cope with aminoglycoside stress at both sub-lethal and lethal concentrations of these antibiotics. Through transcriptomic and genetic approaches, we show that *groESL-2* (a specific set of chaperonin-encoding genes located on the second chromosome of *V. cholerae*), are upregulated in cells lacking *vchM* and are needed for the tolerance of *vchM* mutant to lethal aminoglycoside treatment, likely by fighting aminoglycoside-induced misfolded proteins. Interestingly, preventing VchM methylation of the four RCCGGY sites located in *groESL-2* region, leads to a higher expression of these genes in WT cells, showing that the expression of these chaperonins is modulated in *V. cholerae* by DNA methylation.

AUTHOR SUMMARY

Bacteria are organisms with a remarkable ability to adapt to several stress conditions, including to the presence of antibiotics. The molecular mechanisms underlying such adaptation lead, very often, to phenomena like antimicrobial tolerance and resistance, responsible for the frequent failure of antibiotic treatment. The study of these molecular mechanisms is thus an important tool to understand development of antimicrobial resistance in bacteria. In this work, we show that abrogating cytosine DNA methylation in *Vibrio cholerae* increases its tolerance to aminoglycosides, a class of antibiotics that cause protein misfolding. DNA methylation is known to affect gene expression and regulate several cellular processes in bacteria. Here we provide evidence that DNA methylation also has a more direct role in controlling antibiotic susceptibility in bacteria. Consequently, the study of bacterial DNA methyltransferases and DNA methylation should not be overlooked when addressing the problem of antimicrobial tolerance/resistance.

INTRODUCTION

In the past decades, the over/misuse and large-scale production of antibiotics has created a serious ecological problem with important consequences for the emergence of antimicrobial resistance (AMR). In fact, a large proportion of the antibiotics ingested are released intact in the environment (1, 2) and found at trace levels or as gradients in various environments (3, 4). Hence, in these environments, one can find the presence of very low

doses of drugs commonly referred as subMIC, i.e. under the MIC (Minimal Inhibitory Concentration). Although not enough to kill or prevent the growth of bacterial populations, subMIC doses of antibiotics are proposed to work as signaling molecules (5) and trigger important stress mechanisms that often result in development of antibiotic resistance (4, 6–8). We have previously shown that subMIC of antibiotics, such as aminoglycosides, trigger common and specific stress responses in Gram-negative bacteria (9, 10).

Aminoglycosides (AGs) are positively charged molecules that bind 16S rRNA at the 30S ribosomal subunit and negatively affect translation. Specifically, AGs (e.g. tobramycin, streptomycin, kanamycin, gentamicin and neomycin) are known to disrupt translational fidelity and increase the levels of mistranslation, i.e. the misincorporation of certain amino acids in proteins (11, 12). In turn, high levels of mistranslation result in the production and accumulation of aberrant proteins in the cell, which contribute to the collapse of important cell processes and ultimately lead to cell death (13, 14).

V. cholerae is a water-borne gram-negative bacterium, human pathogen and the causative agent of cholera disease. As part of its life cycle, *V. cholerae* often transits between the human gut and the external environment where it can find low doses of antibiotics. During our studies to better understand adaption of *V. cholerae* to aminoglycosides (15), we observed that a mutant of a *V.* cholerae's specific DNA methyltransferase (*vca0198* - VchM) was less susceptible to aminoglycosides than its isogenic WT strain, suggesting that DNA methylation could play a role in *V. cholerae* adaptation to AGs. *vchM* codes for an Orphan m5C DNA methyltransferase that causes DNA methylation at 5'-RCCGGY-3' motifs (16). DNA methylation is catalyzed by enzymes called

DNA methyltransferases (DNA MTases) that transfer a methyl group from S-adenosyl-L methionine (SAM) to adenine and cytosine in specific DNA motifs (17, 18). As a result, one can find the existence of small amounts of N6-methyl-adenine (6mA), C5-methyl-cytosine (5mC) and N4-methyl-cytosine (4mC) in the DNA of both eukaryotes and prokaryotes. In bacteria, the existence of such modified DNA bases have been shown to play a critical role in processes such as protection against invasive DNA, DNA replication and repair, cell cycle regulation and control of gene expression (19–23).

While it was previously proposed that VchM plays a role in the cell envelope stress response of *V. cholerae* (23), no link between this DNA MTase and antibiotic stress has yet been established. Here, we show that deletion of *vchM* (although causing a growth defect in absence of stress) allows *V. cholerae* cells to better deal with the effect of aminoglycosides. In fact, not only the *vchM* mutant is a better competitor during growth in presence of subMIC doses of aminoglycosides, it is also more tolerant to killing by lethal doses of these antibiotics. Transcriptome analysis of a Δ*vchM* strain revealed the upregulation of *groESL-2* genes, a specific set of chaperonin-encoding genes located on the second chromosome of *V. cholerae*. High expression of *groESL-2* genes (but not of chromosome one *groESL-1* homologues) determines the higher tolerance of Δ*vchM* to lethal AG treatment, suggesting a new and specific role of *groESL-2* in managing AG-mediated proteotoxic stress. Interestingly, we observed the presence of four VchM motifs in *groESL-2* region. Preventing methylation of all these sites in the WT strain by disrupting such motifs results in increased expression of these genes. Intriguingly, the high expression of *groESL-2* does not seem to contribute to the competitive advantage of the Δ*vchM* strain

grown under subMIC AG which suggests the involvement of additional players in the global response of Δ*vchM* to aminoglycosides.

RESULTS

V. cholerae cells lacking *vchM* cope better with subMIC doses of AGs

In order to explore a possible role of *vchM* in the response of *V. cholerae* O1 El Tor N16961 to aminoglycosides, we constructed an in-frame deletion mutant of *vchM* by allelic replacement with an antibiotic resistance cassette, and compared its growth to the isogenic wild-type (WT) strain, in rich media, with or without increasing concentrations of subMIC tobramycin (Fig 1). As previously described (23), this mutant exhibits a reduced doubling rate when grown in monoculture in antibiotic free rich media. However, the difference in growth between WT and Δ*vchM* strains observed in absence of antibiotics becomes gradually more negligible with increasing concentrations of subMIC TOB. At higher concentrations (90% of the MIC), Δ*vchM* even displays a clear advantage over the WT (Fig 1A). Importantly, a Δ*vchM* strain harboring a low-copy number plasmid with *vchM* gene under the control of its own promoter behaves as the WT strain in absence of tobramycin and even slightly worse in presence of higher doses of this drug (Fig 1A), showing that the observed growth phenotypes are due to the absence of *vchM*.

Next, we asked whether the growth phenotype observed in monocultures was translatable to a higher relative fitness in co-cultures in the presence of subMIC doses of tobramycin and other AGs. For that, we competed both WT and Δ*vchM* strains (both *lacZ*$^{+}$) with an isogenic *ΔlacZ* mutant (initial ratio of 1:1), in MH or MH supplemented with subMIC concentrations (50% MIC) of the aminoglycosides tobramycin (TOB), gentamicin (GEN) and neomycin (NEO). We assessed relative fitness by plating cultures after 20 hours of growth and counting the final proportion of lacZ^{+}/lacZ^{-} colonies. Competition of WT against the *lacZ*$^{-}$ mutant served as a control to account for any effect of *lacZ* deletion on growth. Supporting the previous results in monocultures, Δ*vchM* is outcompeted by the *lacZ* mutant in MH (≈10-fold difference) (Fig 1B). More importantly, in presence of low concentrations of aminoglycosides, Δ*vchM* is either equally competitive or even displays a clear growth advantage over the reference strain (Fig 1B). Additionally, in order to test whether these results hold for drugs other than aminoglycosides we performed competitions in the presence of chloramphenicol (CAM) and the beta-lactam carbenicillin (CARB). Unlike AGs, the presence of low concentrations of these drugs did not increased the relative fitness of the Δ*vchM* mutant.

Altogether, these results confirm that lack of *vchM* in *V. cholerae* negatively impacts growth in antibiotic-free media (23) but confers a selective advantage to *V. cholerae* in presence of subMIC doses of AGs (Fig 1). In order to test if deleting *vchM* affects the MIC of these drugs, we measured the MIC of both WT and Δ*vchM* mutant and found no difference (Table 1).

Table 1. MICs (μg/ml) of the different antibiotics tested for *V. cholerae* N16961 WT and *ΔvchM* strains

Strain	TOB	GEN	NEO	CAM	CARB
WT	1-2	1	4	1	15
Δ*vchM*	1-2	1	4	1	7.5

TOB, tobramycin; GEN, gentamicin; NEO, neomycin; CAM, chloramphenicol; CARB, carbenicillin

VchM deficiency promotes higher tolerance to lethal doses of aminoglycosides

It has been previously shown that certain mutations affect functions conferring bacterial populations a tolerant phenotype towards a specific drug (24). Such bacterial populations can transiently withstand lethal doses of that drug without necessarily any impact on the MIC of the population (24).

To continue exploring the different susceptibility of the Δ*vchM* strain to aminoglycosides we assessed the survival rate of *V. cholerae* WT and Δ*vchM* strains during treatment with lethal doses of tobramycin and gentamicin at 20x and 10x the MIC, respectively (Fig 2). Given the inherent growth defect of VchM deficiency, we performed time-dependent killing curves on stationary phase cells, where both WT and Δ*vchM* strains are no longer actively growing, excluding a possible link between growth rate and aminoglycoside lethality as previously shown (25). Strikingly, survival to both antibiotics was increased 10-1000 fold in the Δ*vchM* mutant, suggesting that the absence of VchM allows *V. cholerae* to transiently withstand lethal doses of these aminoglycosides (Fig 2). We additionally tested the

tolerance of exponential phase cells of WT and Δ*vchM* mutant strains to lethal concentrations of tobramycin and observed similar results (S1 Fig).

One crucial aspect that determines the efficacy of aminoglycoside treatment is the uptake of these drugs by the bacterial cell. This process is energy dependent and requires a threshold membrane potential (26). We used a previously reported assay that measures cell fluorescence after incubation with fluorescent-marked neomycin (neo-cy5) (27) as a proxy for aminoglycoside uptake. We did not observe any difference in fluorescence between WT and Δ*vchM* mutant strains (S2 Fig). Thus, differential uptake of aminoglycosides is unlikely the reason for the increased tolerance to these drugs in Δ*vchM*.

A specific set of chaperonins is upregulated in *ΔvchM* cells

To understand the high tolerance to aminoglycosides observed in Δ*vchM*, we performed RNA-seq on stationary phase cells of WT and Δ*vchM* strains grown in rich, stress-free media. The analysis of the transcriptome of Δ*vchM V. cholerae* O1 El Tor N16961 strain reveals the significant upregulation (fold change ≥ 2, $p<0.01$) and downregulation (fold change ≤ -2, $p<0.01$) of 68 and 53 genes, respectively (S1 Table). Among the differentially expressed, we found four genes directly involved in protein folding to be upregulated in Δ*vchM* strain. Those are the molecular chaperones GroEL and co-chaperonins GroES (Table 2). In many bacterial species, GroEL and its co-chaperonin GroES form a molecular machine essential for folding of large newly synthesized proteins also helping re-folding of proteins

damaged by proteotoxic stress (28). Interestingly, overexpression of GroES and GroEL proteins was found to promote short-term tolerance to aminoglycoside-induced protein misfolding in *E. coli* (29).

Table 2. Protein folding and stabilization genes upregulated in Δ*vchM* (fold change > 2, p-value < 0.01)

Locus	Name	Fold change (Δ*vchM*/WT)	Annotation
vc2665	groEL-1	**2.24**	Chaperonin, 60-kDa subunit
vca0820	groEL-2	**3.54**	Chaperonin, 60-kDa subunit
vc2664	groES -1	**2.60**	Chaperonin, 10-kDa subunit
vca0819	groES-2	**6.78**	Chaperonin, 10-kDa subunit

V. cholerae is one of, at least, seven *Vibrio* species harboring two copies of *groES – groEL* (*groESL*) bicistronic operons (30). Whereas *groESL-1* is encoded in chromosome 1 (*vc2664-vc2665*), *groESL-2* is located in chromosome 2 (*vca0819-0820*) (Fig 3A) (30). Based on our RNA-seq data, the latter manifested a larger fold change (Table 2). In order to confirm differential expression of these genes in Δ*vchM,* we measured *groES-1* and *groES-2* relative gene expression in exponential and stationary phase cells of WT and mutant strains, using digital qRT-PCR with the housekeeping *gyrA* gene as reference (31). The results confirm a higher induction of *groES-2* genes in both exponential and stationary phase Δ*vchM* cells with a fold change (over the WT) of ca. 10X and 5X, respectively (Fig 3B). However, *groES-1* fold change was only slightly increased in exponential and unnoticeable in stationary phase.

Induction of groESL genes is usually associated to perturbations in proteostasis which leads to activation of the heat-shock response (32). Indeed, expression of both

groESL-1 and *groESL-2* is controlled by the heat-shock alternative sigma factor RpoH in *V. cholerae* (33). However, the upregulation of *groESL-2* genes in Δ*vchM* cells is likely independent of heat-shock activation as i) we do not observe any other genes of the heat-shock regulon being upregulated in the mutant (for example, *dnaKJ*/*grpE*, *clpB, ibpAB*) and ii) expression of *groESL-1* is not as increased as expression of *groESL-2* (Fig 3B).

Altogether, these results confirm that in absence of VchM, expression of *groESL-2* genes is markedly increased in *V. cholerae* and suggest that regulation of *groESL-2* operon in the Δ*vchM* mutant can be independent of heat-shock response.

Deletion of *groESL-2* operon abolishes *ΔvchM* high tolerance to lethal doses of tobramycin

In bacteria that harbor a single copy of this operon, GroESL are essential proteins for cell viability (34). However, possible redundancy between *groESL-1* and *groESL-2* could allow for the deletion of one or the other operon in *V. cholerae*. Thus, we attempted to delete *groESL-1* and *groESL-2* from *V. cholerae* WT and Δ*vchM* strains. While Δ*groESL-2* and Δ*vchM groESL-2* strains were easily obtained, we could not manage to delete *groESL-1* in any background despite several attempts. Moreover, deletion of *groESL-2* did not affect the growth of V*. cholerae* in rich medium (Fig 4A). Respectively, GroES-1 and GroEL-1 share 80% and 87% amino acid identity with the only and essential GroES and GroEL proteins of *E. coli*, but lower (66% and 76%) amino acid identity with GroES-2 and GroEL-2 (S3 Fig). These observations suggest that i) GroESL-1 (but not GroESL-2) is essential for *V. cholerae* viability and ii) GroESL-1 is probably the main housekeeping chaperonin system while the divergent

GroESL-2 could act synergistically in response to high levels of misfolding or having specific substrates upon protein damage caused by specific stresses. Surprisingly, competition of Δ*groESL-2* with a lacZ$^-$ strain shows that loss of these proteins is not detrimental for growth of *V. cholerae* in presence of subMIC TOB (S4A Fig). Similarly, survival of the Δ*groESL-2* strain to lethal doses of TOB does not differ from that of the WT (S4B Fig). However, these genes are intrinsically highly expressed in Δ*vchM* strain, where they may confer a selective advantage in presence of AG stress. In this case, deletion of *groESL-2* in Δ*vchM* background would affect the mutant's tolerance. Indeed, when we compared the survival to lethal AG treatment of Δ*vchM* to that of a Δ*vchM groESL-2* double mutant, we found that the absence of *groESL-2* abolishes high tolerance to tobramycin and gentamicin in Δ*vchM* (Fig 4B), without affecting growth in absence of stress (Fig 4A). These results show that the higher expression of *groESL-2* is required for the high tolerance of the Δ*vchM* mutant to lethal AG treatment. Importantly, we assessed whether *groESL-2* locus is part of *V. cholerae*'s intrisinc stress response to AGs, and we observed induction of this locus by both subMIC and lethal concentrations of tobramycin (S5 Fig)"

We then tested whether the high tolerance of this mutant relies on general higher levels of chaperonins or if it specifically linked to GroESL-2 chaperonins. We thus tried to complement the Δ*vchM groESL-2* mutant by ectopically expressing *groESL-1* or *groESL-2* and assessed survival to lethal doses of AGs. Strikingly, only overexpression of *groESL-2* is able to promote survival levels similar to those observed in Δ*vchM* (Fig 4C), suggesting a specific role for GroESL-2 in managing AG-mediated proteotoxic stress in *V. cholerae* cells lacking VchM. Interestingly, we observed no difference in the relative fitness of Δ*vchM* and

Δ*vchM groESL-2* mutants in competitions in presence of subMIC doses of tobramycin, which shows that *groESL*-2 it is not implicated in Δ*vchM* higher relative fitness during growth in subMIC AGs (Fig 4D).

VchM controls *groESL-2* expression in part through direct DNA methylation

Knowing the role of VchM in regulating gene expression in *V. cholerae* (23), we asked whether VchM controls *groESL* expression directly through DNA methylation. VchM methylates the first cytosine in 5'-R**C**CGGY-3' motifs (16). This prompted us to search for such motifs in both *groESL* operons. While we couldn't detect any of these sites along the *groESL-1* locus, we found a total of four VchM motifs in *groESL-2* region: motif #1 within the 5' UTR of the operon, 47 bp away from the initiation codon; motif #2 is within the coding region of *groES-2* while motifs #3 and #4 are located within the coding region of *groEL-2* (Fig 5A). We hypothesized that the methylation state of these motifs could modulate the transcription of *groESL-2* genes. To test this, we generated a mutant by replacing all RCCGGY motifs in *groESL-2* region by non-consensus motifs but maintaining the amino acid sequence of GroESL-2 proteins intact (Fig 5A, mut#1-4). Additionally, we created a mutant where only the RCCGGY #1 was altered in order to investigate if this site, for being in the regulatory region of this operon, had a stronger contribution in modulating gene expression (Fig 5A, mut#1). We then measured *groES-2* expression in both mutants and observed that disruption of RCCGGY #1 lead to a very weak increase in *groES-2* expression relative to the WT, while disruption of all four sites led to a significantly higher expression of this gene (Fig 5B), although not as high as in the *ΔvchM* mutant. We additionally tested *groEL-2* expression and observed similar results (S6 Fig). Supporting our hypothesis that this

277 regulation is methylation-dependent, we did not observe any difference in *groES-2* or
278 *groEL-2* expression when we mutated sites #1-4 in the Δ*vchM* background (S6 Fig). It is
279 worth mentioning that, in these experiments, the expression of *groES-2* in the Δ*vchM* strain
280 was consistently higher than in the WT mut#1-4 (Fig 5B) suggesting that an additional factor
281 (e.g. an unknown DNA methylation-sensitive transcription factor), in synergy with the
282 methylation of RCCGGY sites, controls expression of *groES-2*. Nonetheless, overall these
283 results show that a specific set of chaperonin encoding genes is under the control of DNA
284 cytosine methylation in *V. cholerae*, linking DNA methylation to modulation of chaperonin
285 expression and tolerance to antibiotics.

286

287

288 **DISCUSSION**

289 Antimicrobial resistance (AMR) is currently one of the biggest threats to global
290 health (35). It is thus urgent to not only find new and alternative ways to fight bacterial
291 infections but also to understand how bacteria adapt to the presence of antibiotics and
292 study the molecular mechanisms they use to circumvent antibiotic action.

293 In this study, we establish a previously unknown link between VchM-mediated DNA
294 methylation and aminoglycoside susceptibility in the human pathogen *V. cholerae*. VchM is
295 a relatively understudied orphan DNA methyltransferase only found in *V. cholerae* species,
296 known to methylate the first cytosine at 5'-RCCGGY-3' DNA motifs (16, 23). VchM is
297 necessary for the optimal growth of *V. cholerae*, both *in vitro* and *in vivo*, and it was shown

298 to repress the expression of a gene important for cell envelope stability through direct DNA
299 methylation (23).

300 Here we show that despite the growth defect in stress-free medium, cells lacking
301 VchM are also less susceptible to aminoglycoside toxicity. Specifically, we show that these
302 cells have a higher relative fitness in presence of low AG concentrations. The reason for this
303 can be inferred from the growth curves in presence of subMIC TOB (Fig 1A) where it is clear
304 that small increments in TOB concentration lead to a higher toxicity in the WT strain when
305 compared to the Δ*vchM*. Moreover, even though the MIC values for the tested AGs are the
306 same in both strains, Δ*vchM* displays a higher tolerance to lethal aminoglycoside treatment
307 (Fig 2).

308 Aminoglycosides are a well-known class of antimicrobial drugs that cause disruption
309 of the translation process and consequently protein misfolding (14, 36). The exact
310 mechanism underlying the bactericidal activity of aminoglycosides has been subject of
311 debate in the literature (37) but it is generally accepted that killing by AGs involves i) the
312 uptake of the AG into the cytoplasm (11, 38, 39) and ii) membrane disruption mediated by
313 insertion of misfolded proteins in the membrane as consequence of AG binding to the
314 ribosomes and disruption of translational fidelity (11–13, 40). Indeed, mechanisms
315 modulating aminoglycoside tolerance/resistance in different bacterial species (in
316 exponential or stationary phase) have been shown to be associated either to AG uptake
317 (41–44) or to translational fidelity and proteostasis (14, 29, 40, 45). Our results revealed a
318 higher relative abundance of *groESL-2* transcripts in bacterial cells lacking VchM, which led
319 us to hypothesize that such increased expression of these chaperonins could underlie the

high tolerance to AGs observed in this mutant, as it had been previously observed in *E. coli* (29). In fact, we show that stationary phase cells lacking both *vchM* and *groESL-2* genes have similar or even lower tolerance to lethal AG treatment compared to the WT strain. However, we could not observe a significant increase in tolerance upon overexpression of *groESL-2* in the WT strain (S7 Fig), suggesting that high *groESL-2* levels alone do not explain the high tolerance to lethal AG treatment. Instead, it is possible that high levels of GroESL-2 chaperone system counteract AG-mediated misfolding of specific substrates present only in cells devoid of VchM.

V. cholerae harbors two copies of *groESL* operon in its genome, thus belonging to the group of 30% of bacterial species that contains multiple copies of these chaperonins (46, 47). An interesting question to ask is whether these extra copies of chaperonins are functionally redundant or have a more specialized role in the cell, as it had been observed for *Myxococcus xanthus* (46–48). Supporting the latter hypothesis, we show here that the high tolerance observed in Δ*vchM* is dependent on the high expression of *groESL-2* but not on the high expression of *groESL-1* (Fig 4B). Amino acid identity comparison between these proteins suggests that *Vc* GroESL-1 is likely the orthologue of the housekeeping GroESL of *E. coli* whereas *Vc* GroESL-2, thought to have appeared by duplication in *V. cholerae* (30), differ equally from both (S3 Fig). Thus, we speculate that *V. cholerae* GroESL-2 constitutes an alternative chaperone system capable of helping the folding of specific substrates important for survival to specific stresses. The existence of an alternative *groESL-2* locus in *V. cholerae* that is needed for aminoglycoside tolerance only in certain contexts is a new finding and it paves the way for the study of potential alternative roles of otherwise thought

redundant chaperonin systems in bacteria. It would be interesting, in future studies, to assess in depth how GroESL-2 interacts with specific substrates and which stress conditions demand one of the chaperonins in preference to the other.

Interestingly, even though essential for the higher tolerance to lethal aminoglycoside treatment, *groESL-2* is not involved in the increased relative fitness of the Δ*vchM* mutant in presence of subMIC doses of aminoglycosides (Fig 4C). This suggests that the mechanisms operating in Δ*vchM* cells that increase their relative fitness during growth in subMIC AGs are not the same that increase their tolerance to lethal doses of these drugs. In fact, it has been recently shown that the type of translation errors occurring at lower streptomycin (another AG) concentrations differ from those found in high concentrations of this aminoglycoside, with the latter being associated to a higher misfolding propensity (12). Thus, it seems plausible that, in Δ*vchM* cells, the higher expression of *groESL-2* is likely to be more important at high concentrations of AGs, when the abundance of misfolded proteins tend to increase. The mechanisms driving Δ*vchM* higher relative fitness at lower doses of aminoglycosides remain to be elucidated in future work.

DNA methylation controls gene expression through modulation of protein-DNA interactions (49). In most of the cases, the methylated base interferes with the binding of transcription factors and/or the RNA polymerase at the regulatory region of a gene, affecting transcription (50–52). However, there is also evidence that the presence of methylated DNA bases that occur along the coding region of genes could also directly affect their expression in bacteria, even though the precise mechanism is still unknown (20, 22, 23). In eukaryotes, cytosine methylation tends to repress gene expression. A recent study

shedding light on how cytosine methylation affect DNA mechanical properties shows that cytosine methylation stabilizes the DNA helix and slows transcription in eukaryotic cells (53). Thus, a similar m5C-mediated transcriptional hindrance is likely to happen also in prokaryotes. Here we support this view by showing that abrogation of VchM-dependent methylation of cytosines at the four RCCGGY motifs in *groESL-2* region increased its expression in WT cells (Fig 5B). However, this in unlikely the sole mechanism responsible for the high expression of *groESL-2* genes in Δ*vchM* cells, as this mutant has even higher expression levels of *groESL-2*. This suggests that the pleiotropic effects resulting from VchM deficiency also affect, indirectly, the expression of these genes maybe through regulation of a methylation sensitive transcription factor. Thus, VchM controls *groESL-2* expression in part in a direct and in an indirect way.

Our work shows that a *V. cholerae* deletion mutant of the orphan DNA methyltransferase VchM have a general higher tolerance towards aminoglycosides. It remains to be explored whether *V. cholerae* WT cells can modulate VchM expression and, consequently, alter the levels of cytosine methylation. Bisulfite sequencing analysis of *V. cholerae* genome shows that all cytosines within RCCGGY motifs were methylated in *V. cholerae*, during exponential and stationary phases, with the exception of three of these sites which had been previously shown to be constantly undermethylated in this species (54). However, these studies were conducted in cells cultured in LB stress-free media or collected from frozen rabbit cecal fluid, and thus may not reflect the m5C profile of *V. cholerae* during other stress conditions. Moreover, bisulfite sequencing allows for cytosine methylation analysis of the total population at a specific time and thus it is not suitable to detect potential transient changes

386 in small subpopulations of cells. Such changes could be mediated, for example, by altering
387 the levels of VchM through gene expression. Little is known about *vchM* regulation but it
388 was recently shown that the *V. cholerae* quorum sensing low density transcriptional
389 regulator AphA is able to bind the *vchM* region (55) leaving the possibility that *vchM* may
390 be regulated by quorum sensing. Moreover, *vchM* was previously found to be differentially
391 expressed between different stages of human infection (56), suggesting the possibility that
392 modulation of cytosine methylation levels can be adaptative during *V. cholerae*'s life cycle.
393 In line with our work, lowering VchM levels could lead to a trade-off, where low m5C levels
394 would be detrimental for fitness in stress-free contexts, but highly advantageous in
395 presence of specific stress conditions, such as antibiotic exposure.

396 With this study, we show for the first time that in *V. cholerae* (and potentially other
397 clinically relevant species) the high expression of specialized chaperonins are crucial in
398 certain conditions where specific proteins may be affected by AGs. Moreover, we show here
399 that there is a link between chaperonin expression and DNA cytosine methylation, which
400 has not previously been observed, thus linking DNA methylation levels with response to
401 proteotoxic stress.

402

403

404

405

406

407

MATERIALS AND METHODS

Strains, media and culture conditions

V. cholerae was routinely cultured at 37°C in Mueller-Hinton (MH) medium. Plasmids were introduced in *V. cholerae* by electrotransformation. Strains containing the pSC101 plasmid were grown in presence of 100 µg/mL carbenicilin for plasmid maintenance. All *V. cholerae* mutant strains are derived from *Vibrio cholerae* serotype O1 biotype El Tor strain N16961 hapR+. Mutants were constructed by homologous recombination after natural transformation or with a conjugative suicide plasmid as previously described (15, 57–59). Primers, strains and plasmids used in this study, and their constructions, are listed in Table S2. For routine cloning we used chemically competent *E. coli* One Shot TOP10 (Invitrogen). All strains and plasmids were confirmed by sanger sequencing.

Mutation of RCCGGY sites #1-4 in *groESL-2* region

In order to mutate all four RCCGGY sites present in *groESL-2* (*vca0819-0820*) region we generated a DNA fragment (S2 Table) with these sites containing the following nucleotide changes: #1- ACCGGC changed to A**T**CGGC; #2- ACCGGC changed to AC**G**GGC; #3- GCCGGC changed to GC**G**GGC and #4- ACCGGC changed to AC**G**GGC. This fragment was then introduced in *V. cholerae* at the endogenous locus by allelic replacement as described in Table S2.

Growth curves

Overnight cultures from single colonies were diluted 1:100 in Mueller-Hinton (MH) rich media or MH + subMIC antibiotics at different concentrations, in 96-well microplates. OD_{600} was measured in a Tecan Infinite plate reader at 37°C, with shaking for 20 hours. Measurements were taken every 10 minutes.

MIC determination

MICs were determined by microtiter broth dilution method (60) with an initial inoculum size of 10^5 CFUs/mL. The MIC was interpreted as the lowest antibiotic concentration preventing visible growth.

Neo-Cy5 uptake

Quantification of fluorescent neomycin (Neo-cy5) uptake was performed as described (61). Neo-cy5 is an aminoglycoside coupled to the fluorophore Cy5, and has been shown to be active against Gram- bacteria (27). Briefly, overnight cultures were diluted 100-fold in rich MOPS (Teknova EZ rich defined medium). When the bacterial cultures reached an OD_{600} of 0.25, they were incubated with 0.4 µM of Cy5 labeled Neomycin for 15 minutes at 37°C. 10 µL of the incubated culture were then used for flow cytometry, diluting them in 250 µL of

PBS before reading fluorescence. Flow cytometry experiments were performed as described (62). For each experiment, 100000 events were counted on the Miltenyi MACSquant device.

Competitions experiments

Overnight cultures from single colonies of $lacZ^-$ and $lacZ^+$ strains were washed in PBS (Phosphate Buffer Saline) and mixed 1:1 (500µl + 500µl). At this point 100µl of the mix were serial diluted and plated in MH agar supplemented with X-gal (5-bromo-4-chloro-3-indolyl-β-D-galactopyranoside) at 40 µg/mL to assess T0 initial 1:1 ratio. At the same time, 10 µl from the mix were added to 2 mL of MH or MH supplemented with subMIC tobramycin at 0.6µg/mL and incubated with agitation at 37°C for 20 hours. Cultures were then diluted and plated in MH agar plates supplemented with X-gal. Plates were incubated overnight at 37°C and the number of blue and white CFUs was assessed. Competitive index was calculated by dividing the number of blue CFUs ($lacZ^+$ strain) by the number of white CFUs ($lacZ^-$ strain) and normalizing this ratio to the T0 initial ratio.

Survival assays

Bacterial cultures from single colonies were cultured at 37°C for 16 h with agitation in 10 mL of MH medium. Aliquots from these cultures were removed, serial diluted and plated in MH agar plates to assess CFUs formation prior antibiotic treatment (T0). In addition, 5 mL of these aliquots were subjected to antibiotic treatment and incubated with agitation at

37°C. At the indicated time points, 500uL of these cultures were collected, washed in PBS, serial diluted and plated in MH agar plates. The plates were then incubated overnight at 37°C. Survival at each time point was determined by dividing the number of CFUs/mL at that time point by the number of CFUs/mL prior treatment. Antibiotics were used at the following final concentrations: 20 μg/mL Tobramycin (TOB) and 10 μg/mL Gentamicin (GEN). Experiments were repeated at least two to three times.

Digital qRT-PCR

For RNA extraction, overnight cultures of three biological replicates of strains of interest were diluted 1:1000 in MH media and grown with agitation at 37°C until an OD_{600} of 0.3 (exponential phase) or an OD_{600} of 1.0 or 2.0 (stationary phase). 0.5 mL of these cultures were centrifuged and supernatant removed. Pellets were homogenized by resuspension with 1.5 mL of cold TRIzol Reagent. Next, 300 μL chloroform were added to the samples following mix by vortexing. Samples were then centrifuged at 4°C for 10 minutes. Upper (aqueous) phase was transferred to a new 2mL tube and mixed with 1 volume of 70% ethanol. From this point, the homogenate was loaded into a RNeasy Mini kit (Quiagen) column and RNA purification proceeded according to the manufacturer's instructions. Samples were then subjected to DNase treatment using TURBO DNA-free Kit (Ambion) according to the manufacturer's instructions. RNA concentration of the samples was measured with NanoDrop spectrophotometer and diluted to a final concentration of 1-10 ng/μL.

qRT-PCR reactions were prepared with 1 µL of diluted RNA samples using the qScript XLT 1-Step RT-qPCR ToughMix (Quanta Biosciences, Gaithersburg, MD, USA) within Sapphire chips. Digital PCR was conducted on a Naica Geode (programmed to perform the sample partitioning step into droplets, followed by the thermal cycling program suggested in the user's manual. Primer and probe sequences used in digital qRT-PCR reaction are listed in Table S3. Image acquisition was performed using the Naica Prism3 reader. Images were then analyzed using Crystal Reader software (total droplet enumeration and droplet quality control) and the Crystal Miner software (extracted fluorescence values for each droplet). Values were normalized against expression of the housekeeping gene *gyrA* as previously described (31).

RNA-seq

For RNA extraction, overnight cultures of three biological replicates of WT and Δ*vchM* strains were diluted 1:100 in MH medium and grown with agitation at 37°C until cultures reach an OD_{600} of 2.0. Total RNA extraction, library preparation, sequencing and analysis were performed as previously described (63). The data for this RNA-seq study has been submitted in the GenBank Sequence Read Archive (SRA) under project number PRJNA509113.

ACKNOWLEDGMENTS

We are thankful to Manon Lang for her valuable help with the neo-cy5 uptake experiments, Dominique Fourmy for the gift of neo-Cy5, and Sebastian Aguilar Pierlé for help with RNAseq analysis. We thank Claudia Chica and Christophe Becavin (Bioinformatics and Biostatistics Hub, Department of computational biology, USR 3756 CNRS, Institut Pasteur) for DNA bisulfite sequencing analysis on stationary phase cultures. We also thank Evelyne Krin for help with molecular cloning procedures and João Gama for helpful comments on the manuscript.

FIGURE CAPTIONS

Fig 1. *V. cholerae* N16961 Δ*vchM* is less susceptible to subMIC aminoglycosides A. Growth curves in absence (MH) or presence of subMIC doses of tobramycin. Bars represent SD (n=3) **B.** *In vitro* competitions of WT and mutant strains against isogenic Δ*lacZ* reference strain in absence or presence of different antibiotics at subMIC concentrations (TOB, 0.6 µg/ml; GEN, 0.5 µg/ml; NEO, 2.0 µg/ml; CAM, 0.4 µg/ml; CARB, 2.5 µg/ml). Box plots indicate the median and the 25th and 75th percentiles; whiskers indicate the min and max values (n=6).

Fig 2. Δ*vchM* strain is more tolerant to lethal aminoglycoside treatment. Survival of stationary-phase WT and Δ*vchM* cells exposed to lethal doses of tobramycin (TOB) **(A)**, and gentamicin (GEN) **(B)**. Survival represents the number of bacteria (CFU/mL) after treatment

532 divided by the initial number of bacteria prior treatment. Time in the X-axis represents the
533 duration of the antibiotic treatment in hours. Means and SD are represented, n=3.

534 **Fig 3. *groESL-2* operon is upregulated in Δ*vchM* strain. A.** Schematic representation of both
535 *groESL* operons in *V. cholerae*. The four RCCGGY sites present along the *groESL-2* region are
536 represented by the inverted orange triangles. **B.** Fold change (Δ*vchM*/WT) of the relative
537 expression levels of *groES-1* and *groES-2* in cultures at exponential phase (Exp, OD_{600} ≈ 0.3)
538 or stationary phase (Stat, OD_{600} ≈ 1.8-2.0). Means and SD are represented, n=3.

539 **Fig 4. *groESL-2* is needed for the increased tolerance of *ΔvchM* to lethal AG treatment. A.**
540 Growth curves in MH medium. Means and SD are represented, n=3. **B.** Survival of
541 stationary-phase WT and Δ*groESL-2* cells exposed to lethal aminoglycoside treatment for 7
542 hours. Box plots indicate the median and the 25th and 75th percentiles; whiskers indicate the
543 min and max values (n=6 from two independent experiments). **C.** Survival (after 7 hours AG
544 treatment) of Δ*vchM groESL-2* double mutant harboring an empty plasmid or a plasmid
545 expressing either *groESL-1* or *groESL-2*, relative to survival of the Δ*vchM* with the control
546 plasmid. Box plots indicate the median and the 25th and 75th percentiles; whiskers indicate
547 the min and max values (n=6 from two independent experiments). In **B** and **C** statistically
548 significant differences were determined using Friedman's test with Dunn's post-hoc test for
549 multiple comparisons. * P<0.05, ** P<0.01, ns = not significant. **D.** *In vitro* competitions of
550 Δ*vchM* and Δ*vchM groESL-2* double mutant strains against isogenic Δ*lacZ* reference strain
551 in absence or presence of subMIC TOB, 0.6 μg/ml; Error bars indicate SD (n=6).

Fig 5. Disrupted VchM sites in *groESL-2* region leads to increased gene expression in the WT. A. Schematic representation of mutants with abrogated VchM sites. **B.** Relative expression of *groES-2* in the different strains at OD_{600} of 1.0. Box plots indicate the median and the 25th and 75th percentiles; whiskers indicate the min and max values (n= 5). Statistical significance was determined by Kruskal-Wallis test with Dunn's post-hoc test for multiple comparisons. * P<0.05, ** P<0.01, ns = not significant

REFERENCES

1. Liu YC, Huang WK, Huang TS, Kunin CM. 1999. Detection of antimicrobial activity in urine for epidemiologic studies of antibiotic use. J Clin Epidemiol, 52(6), 539-545.

2. Haggard BE, Bartsch LD. 2009. Net Changes in Antibiotic Concentrations Downstream from an Effluent Discharge. J Environ Qual, 38(1), 343-352.

3. Fick J, Söderström H, Lindberg RH, Phan C, Tysklind M, Larsson DGJ. 2009. Contamination of surface, ground, and drinking water from pharmaceutical production. Environ Toxicol Chem, 28(12), 2522-2527.

4. Andersson DI, Hughes D. 2014. Microbiological effects of sublethal levels of antibiotics. Nat Rev Microbiol, 12(7), 465-478.

5. Davies J, Spiegelman GB, Yim G. 2006. The world of subinhibitory antibiotic

572 concentrations. Curr Opin Microbiol 9:445–453.

573 6. Wistrand-Yuen E, Knopp M, Hjort K, Koskiniemi S, Berg OG, Andersson DI. 2018.
574 Evolution of high-level resistance during low-level antibiotic exposure. Nat Commun.
575 9(1), 1-12.

576 7. Jørgensen KM, Wassermann T, Jensen PØ, Hengzuang W, Molin S, Høiby N, Ciofu O.
577 2013. Sublethal ciprofloxacin treatment leads to rapid development of high-level
578 ciprofloxacin resistance during long-term experimental evolution of Pseudomonas
579 aeruginosa. Antimicrob Agents Chemother, 57(9), 4215-4221.

580 8. Gullberg E, Cao S, Berg OG, Ilbäck C, Sandegren L, Hughes D, Andersson DI. 2011.
581 Selection of resistant bacteria at very low antibiotic concentrations. PLoS Pathog,
582 7(7), e1002158.

583 9. Baharoglu Z, Mazel D. 2011. Vibrio cholerae triggers SOS and mutagenesis in
584 response to a wide range of antibiotics: A route towards multiresistance. Antimicrob
585 Agents Chemother, 55(5), 2438-2441.

586 10. Baharoglu Z, Babosan A, Mazel D. 2014. Identification of genes involved in low
587 aminoglycoside-induced SOS response in Vibrio cholerae: A role for transcription
588 stalling and Mfd helicase. Nucleic Acids Res, 42(4), 2366-2379.

589 11. Davis BD. 1987. Mechanism of bactericidal action of aminoglycosides. Microbiol Rev,
590 51(3), 341-350.

591 12. Wohlgemuth I, Garofalo R, Samatova E, Günenç AN, Lenz C, Urlaub H, Rodnina M V.

2021. Translation error clusters induced by aminoglycoside antibiotics. Nat Commun, 12(1), 1-14.

13. Kohanski MA, Dwyer DJ, Wierzbowski J, Cottarel G, Collins JJ. 2008. Mistranslation of Membrane Proteins and Two-Component System Activation Trigger Antibiotic-Mediated Cell Death. Cell, 135(4), 679-690.

14. Ling J, Cho C, Guo LT, Aerni HR, Rinehart J, Söll D. 2012. Protein Aggregation Caused by Aminoglycoside Action Is Prevented by a Hydrogen Peroxide Scavenger. Mol Cell 48:713–722.

15. Negro V, Krin E, Pierlé SA, Chaze T, Gianetto QG, Kennedy SP, Matondo M, Mazel D, Baharoglu Z. 2019. RadD contributes to R-Loop avoidance in Sub-MIC tobramycin. MBio, 10(4), e01173-19.

16. Banerjee S, Chowdhury R. 2006. An orphan {DNA} (cytosine-5-)-methyltransferase in Vibrio cholerae 152:1055–1062.

17. Fujimoto D, Srinivasan PR, Borek E. 1965. On the Nature of the Deoxyribonucleic Acid Methylases. Biological Evidence for the Multiple Nature of the Enzymes. Biochemistry, 4(12), 2849-2855.

18. Casadesús J, Low D. 2006. Epigenetic Gene Regulation in the Bacterial World. Microbiol Mol Biol Rev, 70(3), 830-856.

19. Sánchez-Romero MA, Casadesús J. 2020. The bacterial epigenome. Nat Rev Microbiol, 18(1), 7-20.

20. Kumar S, Karmakar BC, Nagarajan D, Mukhopadhyay AK, Morgan RD, Rao DN. 2018. N4-cytosine DNA methylation regulates transcription and pathogenesis in Helicobacter pylori. Nucleic Acids Res, 46(7), 3429-3445.

21. Estibariz I, Overmann A, Ailloud F, Krebes J, Josenhans C, Suerbaum S. 2019. The core genome m5C methyltransferase JHP1050 (M.Hpy99III) plays an important role in orchestrating gene expression in Helicobacter pylori. Nucleic Acids Res 47:2336–2348.

22. Militello KT, Simon RD, Qureshi M, Maines R, van Horne ML, Hennick SM, Jayakar SK, Pounder S. 2012. Conservation of Dcm-mediated cytosine DNA methylation in Escherichia coli. FEMS Microbiol Lett, 328(1), 78-85.

23. Chao MC, Zhu S, Kimura S, Davis BM, Schadt EE, Fang G, Waldor MK. 2015. A Cytosine Methytransferase Modulates the Cell Envelope Stress Response in the Cholera Pathogen 11:e1005666.

24. Brauner A, Fridman O, Gefen O, Balaban NQ. Distinguishing between resistance, tolerance and persistence to antibiotic treatment. Nat Rev Microbiol, 14(5), 320-330.

25. Haugan MS, Løbner-Olesen A, Frimodt-Møller N. 2019. Comparative activity of ceftriaxone, ciprofloxacin, and gentamicin as a function of bacterial growth rate probed by Escherichia coli chromosome replication in the mouse peritonitis model. Antimicrob Agents Chemother, 63(2), e02133-18.

26. Nakae R, Nakae T. 1982. Diffusion of aminoglycoside antibiotics across the outer membrane of Escherichia coli. Antimicrob Agents Chemother, 22(4), 554-559.

633 27. Sabeti Azad M, Okuda M, Cyrenne M, Bourge M, Heck MP, Yoshizawa S, Fourmy D.
634 2020. Fluorescent Aminoglycoside Antibiotics and Methods for Accurately
635 Monitoring Uptake by Bacteria. ACS Infect Dis, 6(5), 1008-1017.

636 28. Hartl FU, Hayer-Hartl M. 2002. Protein folding. Molecular chaperones in the cytosol:
637 From nascent chain to folded protein. Science, 295(5561), 1852-1858.

638 29. Goltermann L, Good L, Bentin T. 2013. Chaperonins fight aminoglycoside-induced
639 protein misfolding and promote short-term tolerance in Escherichia coli. J Biol Chem,
640 288(15), 10483-10489.

641 30. Chowdhury N, Kingston JJ, Brian Whitaker W, Carpenter MR, Cohen A, Fidelma Boyd
642 E. 2014. Sequence and expression divergence of an ancient duplication of the
643 chaperonin groESEL operon in Vibrio species. Microbiol (United Kingdom) 160:1953–
644 1963.

645 31. Lo Scrudato M, Blokesch M. 2012. The regulatory network of natural competence
646 and transformation of Vibrio cholerae. PLoS Genet, 8(6), e1002778.

647 32. Richter K, Haslbeck M, Buchner J. 2010. The Heat Shock Response: Life on the Verge
648 of Death. Mol Cell, 40(2), 253-266.

649 33. Slamti, L., Livny, J., & Waldor, M. K. 2007. Global gene expression and phenotypic
650 analysis of a Vibrio cholerae rpoH deletion mutant. Journal of bacteriology, 189(2),
651 351-362.

652 34. Fayet O, Ziegelhoffer T, Georgopoulos C. 1989. The groES and groEL heat shock gene

products of Escherichia coli are essential for bacterial growth at all temperatures. J Bacteriol 171:1379–1385.

35. O'Neill J. 2015. Tackling a Crisis for the Health and Wealth of Nations. Rev Antimicrob Resist.

36. Magnet S, Blanchard JS. 2005. Molecular insights into aminoglycoside action and resistance. Chem Rev 105:477–497.

37. Baquero F, Levin BR. 2021. Proximate and ultimate causes of the bactericidal action of antibiotics. Nat Rev Microbiol, 19(2), 123-132.

38. Ezraty B, Vergnes A, Banzhaf M, Duverger Y, Huguenot A, Brochado AR, Su SY, Espinosa L, Loiseau L, Py B, Typas A, Barras F. 2013. Fe-S cluster biosynthesis controls uptake of aminoglycosides in a ROS-less death pathway. Science, 340(6140), 1583-1587.

39. Bruni GN, Kralj JM. 2020. Membrane voltage dysregulation driven by metabolic dysfunction underlies bactericidal activity of aminoglycosides. Elife, 9, e58706.

40. Zou J, Zhang W, Zhang H, Zhang XD, Peng B, Zheng J. 2018. Studies on aminoglycoside susceptibility identify a novel function of KsgA to secure translational fidelity during antibiotic stress. Antimicrob Agents Chemother 62:1–13.

41. Shan Y, Lazinski D, Rowe S, Camilli A, Lewis K. 2015. Genetic basis of persister tolerance to aminoglycosides in Escherichia coli. MBio 6:1–10.

42. Allison KR, Brynildsen MP, Collins JJ. 2011. Metabolite-enabled eradication of

673 bacterial persisters by aminoglycosides. Nature, 473(7346), 216-220.

674 43. McKay SL, Portnoy DA. 2015. Ribosome hibernation facilitates tolerance of
675 stationary-phase bacteria to aminoglycosides. Antimicrob Agents Chemother
676 59:6992–6999.

677 44. Hall CW, Farkas E, Zhang L, Mah TF. 2019. Potentiation of Aminoglycoside Lethality
678 by C4-Dicarboxylates Requires RpoN in Antibiotic-Tolerant Pseudomonas aeruginosa.
679 Antimicrob Agents Chemother, 63(10), e01313-19.

680 45. Ji X, Zou J, Peng H, Stolle AS, Xie R, Zhang H, Peng B, Mekalanos JJ, Zheng J. 2019.
681 Alarmone Ap4A is elevated by aminoglycoside antibiotics and enhances their
682 bactericidal activity. Proc Natl Acad Sci U S A, 116(19), 9578-9585.

683 46. Kumar CMS, Mande SC, Mahajan G. 2015. Multiple chaperonins in bacteria—novel
684 functions and non-canonical behaviors. Cell Stress Chaperones 20:555–574.

685 47. Goyal K, Qamra R, Mande SC. 2006. Multiple gene duplication and rapid evolution in
686 the groEL Gene: Functional implications. J Mol Evol, 63(6), 781-787.

687 48. Wang Y, Zhang W yan, Zhang Z, Li J, Li Z feng, Tan Z gao, Zhang T tian, Wu Z hong, Liu
688 H, Li Y zhong. 2013. Mechanisms Involved in the Functional Divergence of Duplicated
689 GroEL Chaperonins in Myxococcus xanthus DK1622. PLoS Genet, 9(2), e1003306.

690 49. Casadesus J, Low D. 2006. Epigenetic Gene Regulation in the Bacterial World.
691 Microbiol Mol Biol Rev, 70(3), 830-856.

692 50. Hernday AD, Braaten BA, Low DA. 2003. The mechanism by which DNA adenine

693 methylase and PapI activate the Pap epigenetic switch. Mol Cell, 12(4), 947-957.

694 51. Cota I, Sánchez-Romero MA, Hernández SB, Pucciarelli MG, García-Del Portillo F,
695 Casadesús J. 2015. Epigenetic Control of Salmonella enterica O-Antigen Chain Length:
696 A Tradeoff between Virulence and Bacteriophage Resistance. PLoS Genet, 11(11),
697 e1005667.

698 52. Wion D, Casadesús J. 2006. N6-methyl-adenine: an epigenetic signal for DNA-protein
699 interactions. Nat Rev Microbiol, 4(3), 183-192.

700 53. Rausch C, Zhang P, Casas-Delucchi CS, Daiß JL, Engel C, Coster G, Hastert FD, Weber
701 P, Cardoso MC. 2021. Cytosine base modifications regulate DNA duplex stability and
702 metabolism. Nucleic Acids Res.

703 54. Dalia AB, Lazinski DW, Camilli A. 2013. Characterization of undermethylated sites in
704 vibrio cholerae. J Bacteriol, 195(10), 2389-2399.

705 55. Haycocks JRJ, Warren GZL, Walker LM, Chlebek JL, Dalia TN, Dalia AB, Grainger DC.
706 2019. The quorum sensing transcription factor AphA directly regulates natural
707 competence in Vibrio cholerae. PLoS Genet, 15(10), e1008362.

708 56. LaRocque RC, Harris JB, Dziejman M, Li X, Khan AI, Faruque ASG, Faruque SM, Nair
709 GB, Ryan ET, Qadri F, Mekalanos JJ, Calderwood SB. 2005. Transcriptional profiling of
710 Vibrio cholerae recovered directly from patient specimens during early and late
711 stages of human infection. Infect Immun, 73(8), 4488-4493.

712 57. Baharoglu Z, Krin E, Mazel D. 2012. Connecting environment and genome plasticity

713 in the characterization of transformation-induced {SOS} regulation and carbon
714 catabolite control of the Vibrio cholerae integron integrase. J Bacteriol 194:1659–
715 1667.

716 58. Baharoglu Z, Krin E, Mazel D. 2013. RpoS Plays a Central Role in the SOS Induction by
717 Sub-Lethal Aminoglycoside Concentrations in Vibrio cholerae. PLoS Genet, 9(4),
718 e1003421.

719 59. Val ME, Skovgaard O, Ducos-Galand M, Bland MJ, Mazel D. 2012. Genome
720 engineering in Vibrio cholerae: A feasible approach to address biological issues. PLoS
721 Genet, 8(1), e1002472.

722 60. Name P, Date R. 2010. Methods for Dilution Antimicrobial Suceptibility tests for
723 Bacteria that Grow Aerobically; Approved Standard- Seventh Edition. Clin Lab Stand
724 Inst.

725 61. Lang, M., Krin, E., Korlowski, C., Sismeiro, O., Varet, H., Coppée, J.-Y., Mazel, D.,
726 Baharoglu, Z., Sleeping ribosomes: bacterial signaling triggers RaiA mediated
727 persistence to aminoglycosides., ISCIENCE (2021)

728 62. Baharoglu Z, Bikard D, Mazel D. 2010. Conjugative {DNA} transfer induces the
729 bacterial {SOS} response and promotes antibiotic resistance development through
730 integron activation. {PLoS} Genet 6:e1001165.

731 63. Krin E, Pierlé SA, Sismeiro O, Jagla B, Dillies MA, Varet H, Irazoki O, Campoy S, Rouy
732 Z, Cruveiller S, Médigue C, Coppée JY, Mazel D. 2018. Expansion of the SOS regulon
733 of Vibrio cholerae through extensive transcriptome analysis and experimental

734 validation. BMC Genomics, 19(1), 1-18.

735

736

737 **SUPPORTING INFORMATION**

738 **S1 Table. Differentially regulated genes in ΔvchM strain**

739 **S2 Table. Strains, plasmids and primers used in this study**

740 **S3 Table. Primer and probe sequences used in digital qRT-PCR**

741 **S1 Fig. Δ*vchM* exponential phase cells are more tolerant to lethal aminoglycoside**
742 **treatment.** Survival of exponential phase cells (OD_{600} 0.3-0.4) of WT and Δ*vchM* strains
743 exposed to lethal doses of tobramycin (TOB) for a period of 3.5 hours. The Y-axis represents
744 the $\log_{10}$ CFUs/mL after 3.5 hours growth with 0, 3, 5 or 10 μg/mL of Tobramycin (3x, 5x or
745 10x higher than the MIC, respectively). Means and SD are represented, n=3.

746 **S2 Fig. Neo-cy5 uptake is not decreased in Δ*vchM.*** Percentage of neo-cy5 positive cells
747 analyzed by flow cytometry after incubation with fluorescent marked neomycin. Means and
748 SD are represented, n=3.

749

750 **S3 Fig. Comparison of GroESL proteins from *E. coli* and *V. cholerae.*** Amino acid identity
751 between GroES and GroEL proteins of *E. coli* MG1655 (*Eco*) and *V. cholerae* O1 El Tor
752 N16961 (*Vch*) computed by BLASTP. Values represent percentage identity between
753 proteins.

S4 Fig. Deletion of *groESL-2* does not increase susceptibility to tobramycin. A. *In vitro* competitions of WT and Δ*groESL-2* strains against isogenic Δ*lacZ* reference strain in absence or presence of tobramycin (TOB) at 0.6 μg/mL; n=3, error bars indicate SD. **B.** Survival of stationary-phase WT and Δ*groESL-2* cells exposed to 20X MIC of tobramycin. n=3, error bars indicate SD.

Fig. S5 *groESL-2* is induced in WT cells by tobramycin at both subMIC and lethal concentrations. Relative expression of *groES-2* in WT cells growing in MH, MH with subMIC tobramycin (≈ 20% MIC) or exponential phase cells following lethal TOB treatment (5X MIC) for a period of 30 minutes. n=3, error bars indicate SD.

S6 Fig. Mutation of VchM sites in *groESL-2* region fails to affect gene expression of the operon in absence of VchM. Relative expression of *groES-2 and groEL*-2 genes in the indicated strains grown at OD_{600} 1.0. n=3, error bars indicate SD.

S7 Fig. Overexpression of *groESL-2* in the WT does not increase tolerance to tobramycin. Survival (after 7 hours TOB treatment) of WT strain carrying a control plasmid or a plasmid overexpressing *groESL-2* genes. n=6, error bars indicate SD.

774 **Figure 1**

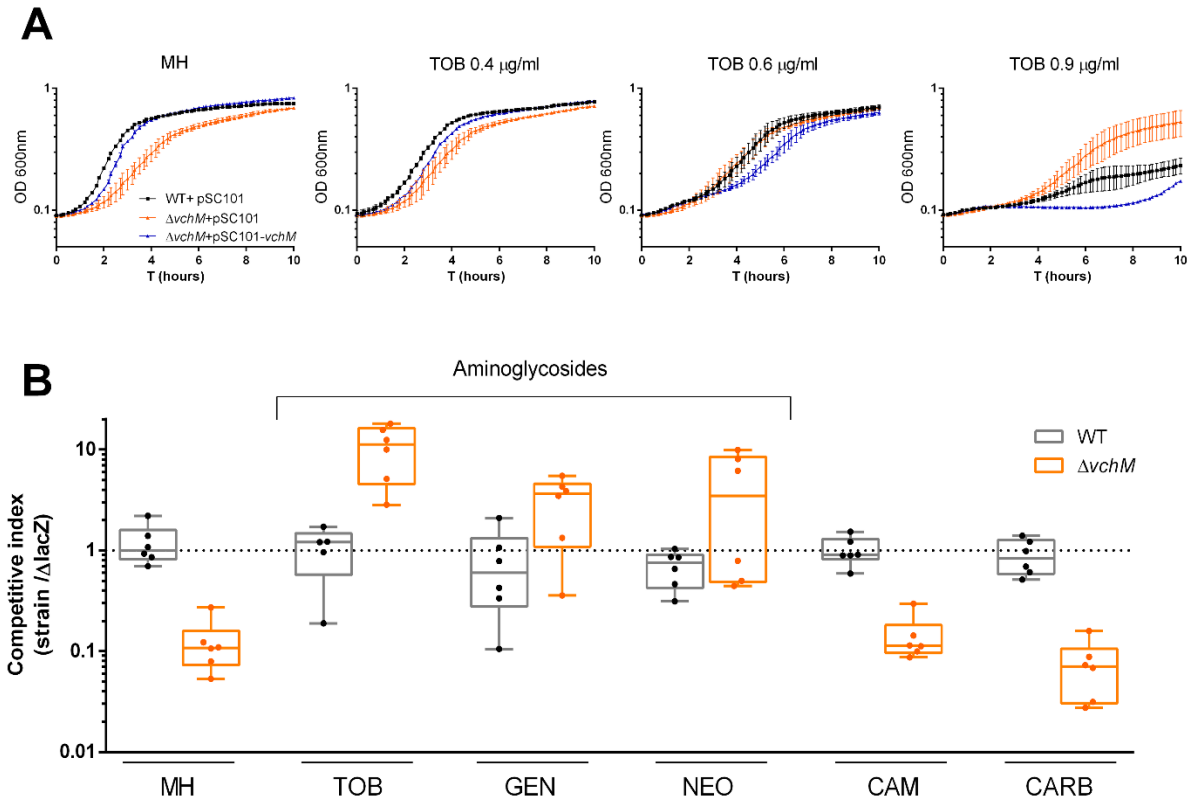

775

776 **Figure 2**

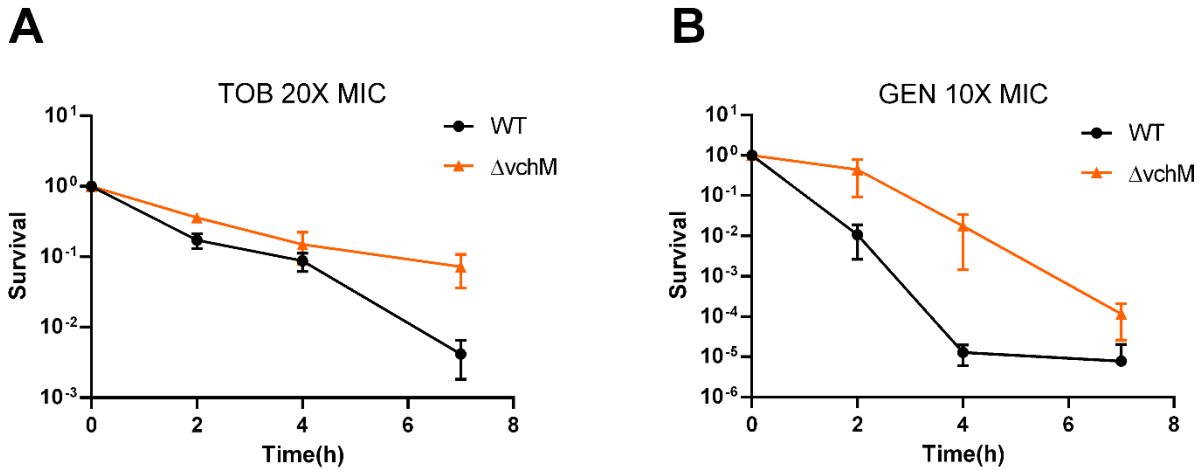

Figure 3

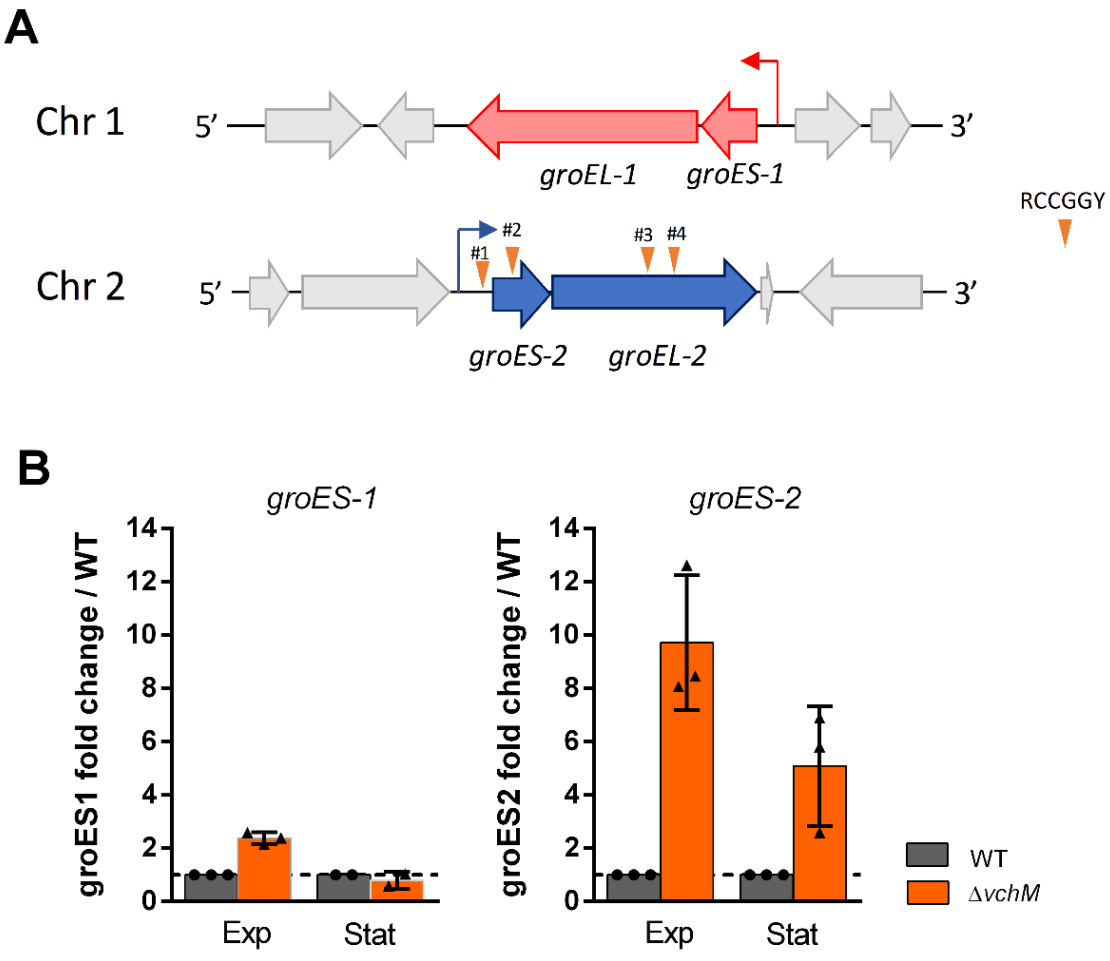
A
Chr 1
5′
3′
groEL-1
groES-1
RCCGGY
Chr 2
#1
#2
#3
#4
5′
3′
groES-2
groEL-2
B
groES-1
groES2 fold change / WT
groES-2
groES1 fold change / WT
14
12
10
8
6
4
2
0
Exp
Stat
WT
ΔvchM

Figure 4

806

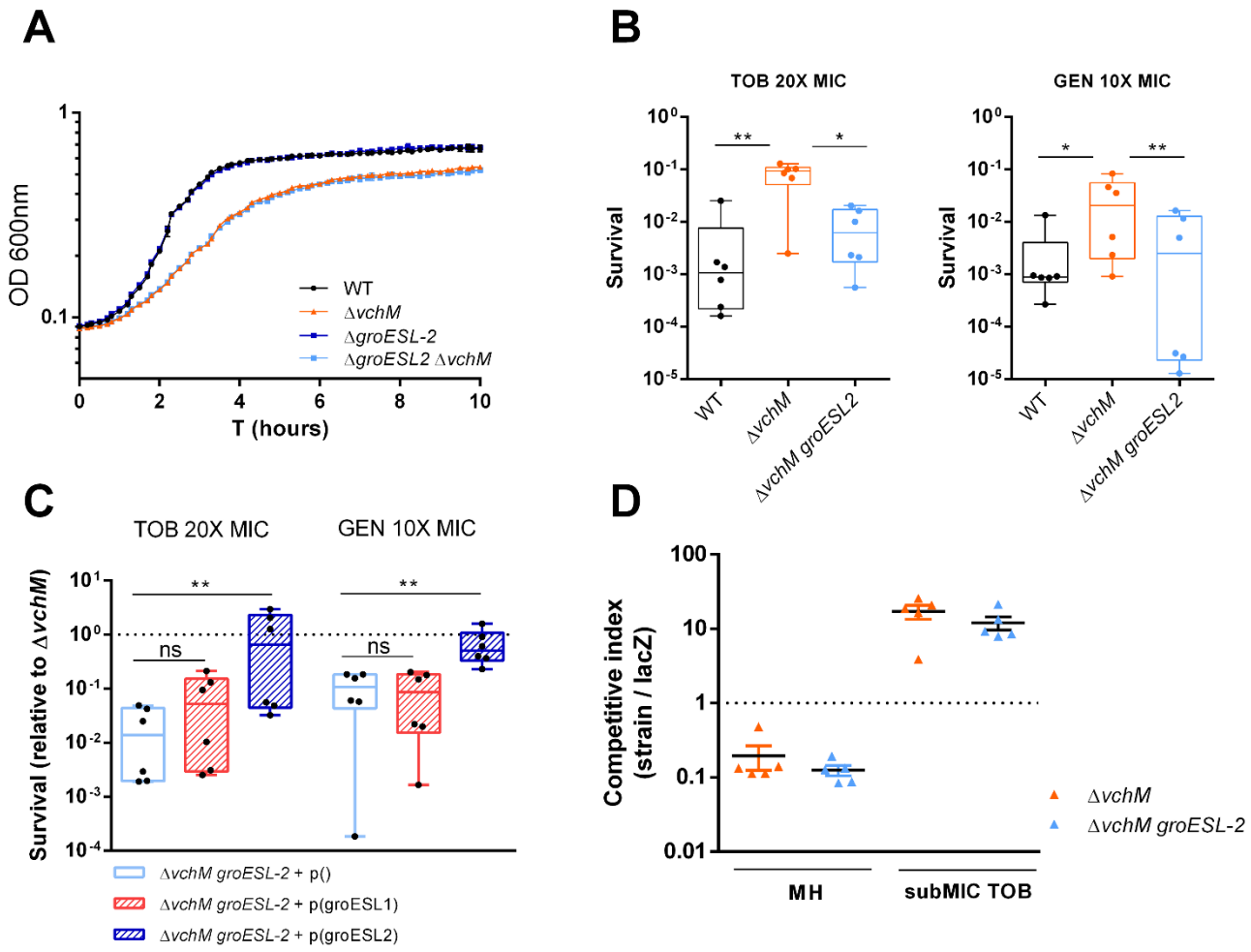

807

808

809

810

811

812

813

814

815

Figure 5

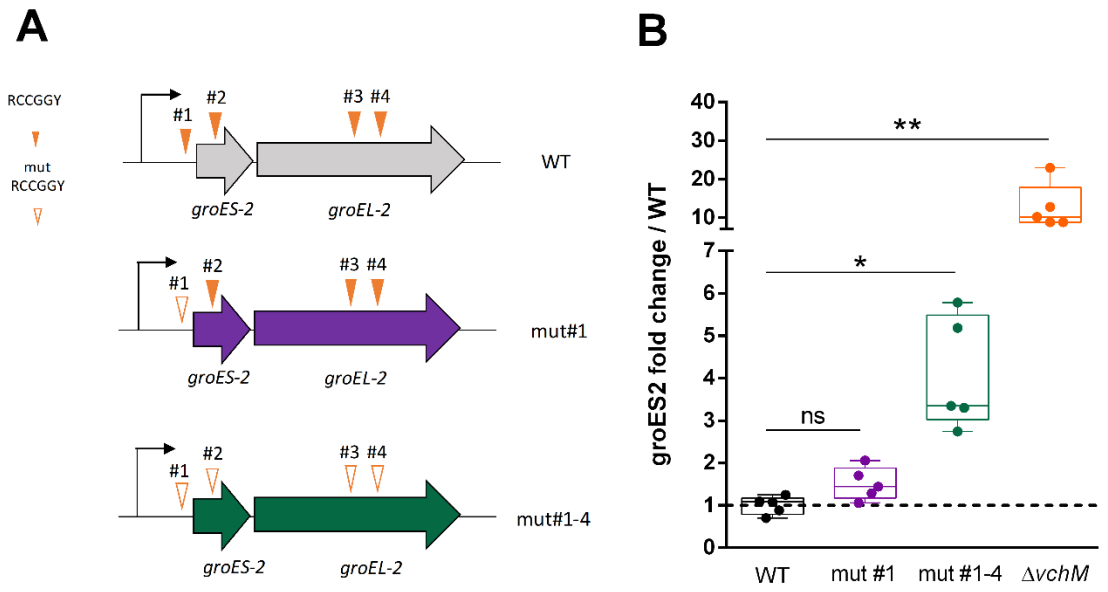

Supplementary data

Table S1. Differentially regulated genes in *ΔvchM* strain

Locus	Name	Annotation	Fold change *ΔvchM*/WT	p-value
UPREGULATED				
vca1028	*lamB*	maltoporin	52,81	0,0E+00
vca0707	*uhpC*	MFS transporter	8,76	8,6E-06
vc1368		conserved hypothetical protein	8,18	0,0E+00
vca0819	***groES-2***	**chaperonin**	**6,78**	**0,0E+00**
vca0200		putative ATPase	6,10	0,0E+00
vca0957	*glcB*	putative Malate synthase	5,97	0,0E+00
vca0199		conserved hypothetical protein	5,32	5,2E-09
vca1027	*malM*	putative Maltose operon periplasmic protein MalM	4,14	0,0E+00
vca0201		conserved hypothetical protein	3,97	3,4E-11
vca0946	*malK*	Maltose/maltodextrin import ATP-binding protein malK	3,91	0,0E+00

vca0469	*higA2*	plasmid stabilization system HigA protein (antitoxin of TA system HigB-HigA)	3,91	0,0E+00
vca0468	*higB2*	plasmid stabilization system HigB protein (toxin of TA system HigB-HigA)	3,90	2,3E-10
vca0945	*malE*	maltose ABC transporter periplasmic binding protein	3,90	0,0E+00
vc1819	*aldA*	Aldehyde dehydrogenase	3,84	1,7E-12
vc1204	*hutG*	putative Formimidoylglutamase HutG (histidine utilization)	3,80	2,2E-16
vc1203	*hutU*	Urocanate hydratase (histidine utilization)	3,60	0,0E+00
vca0820	***groEL-2***	**chaperonin**	**3,54**	**2,2E-16**
vca0692	*secF*	fragment of putative SecD/SecF/SecDF export membrane protein (part 2)	3,48	3,2E-08
vc1809	*alpA*	putative Prophage CP4-57 regulatory protein (AlpA)	3,37	1,8E-09
vc1205	*hutI*	Imidazolonepropionase (histidine utilization)	3,24	1,1E-11
vc1740	*fadE*	acyl coenzyme A dehydrogenase	3,22	5,6E-15
vca0944	*malF*	maltose ABC transporter membrane subunit MalF	3,18	0,0E+00
vc1142	*cspD*	Cold shock-like protein cspD	2,88	0,0E+00
vc2530	*hpf*	putative ribosome hibernation promoting factor HPF/sigma 54 modulation protein	2,83	0,0E+00
vca0948	*yaeO*	putative Rho-specific inhibitor of transcription termination (YaeO)	2,78	0,0E+00
vca0998	*xenB*	Xenobiotic reductase B	2,73	4,4E-06
vc0486	*srlR*	putative Transcriptional regulator of sugar metabolism; DeoR family transcriptional regulator	2,65	9,9E-14
vc1874		putative SpoVR family protein	2,64	0,0E+00
vc1202	*hutH*	Histidine ammonia-lyase	2,61	0,0E+00
vc2265	*groES-1*	chaperonin	2,60	0,0E+00
vc2615		conserved hypothetical protein	2,55	4,6E-10
vc1678	*pspA*	Phage shock protein A	2,48	4,6E-10
vc1183		putative 2OG-Fe dioxygenase	2,43	0,0E+00
vca0470		putative Acetyltransferase	2,43	2,1E-08
vca0324	*relB1*	Plasmid stabilization system protein RelB (Anti Toxin of TA system RelB-RelE)	2,43	1,1E-11
vca0886	*kbl*	glycine C-acetyltransferase	2,40	2,3E-08
vca0185	*arfA*	putative Stalled ribosome alternative rescue factor ArfA	2,39	3,0E-13
vca0958		putative transcriptional regulator	2,38	3,9E-10

vca0013	*malP*	maltodextrin phosphorylase	2,37	3,9E-11
vca0881		conserved hypothetical protein	2,36	1,1E-13
vca0551		conserved hypothetical protein	2,35	0,0E+00
vca0391	*higB1*	Plasmid stabilization system HigB protein (Toxin of TA system HigB-HigA)	2,34	1,5E-10
vca0923	*mlp37*	chemoreceptor Mlp37	2,34	2,2E-12
vc2361	*grcA*	Autonomous glycyl radical cofactor	2,30	0,0E+00
vca0392	*higA1*	Plasmid stabilization system HigA protein (Antitoxin of TA system HigB-HigA)	2,28	0,0E+00
vc0665	*vpsR*	Fis family transcriptional regulator (sigma-54 dependent transcriptional regulator)	2,28	0,0E+00
vca0720	*hnoX*	Heme-Nitric Oxide/Oxygen Binding Protein (H-NOX)	2,27	5,1E-10
vc1433	*uspE*	universal stress protein UspE	2,26	0,0E+00
vc1248	*tar*	putative Methyl-accepting chemotaxis protein	2,25	0,0E+00
vc2264	*groEL-1*	chaperonin	2,24	0,0E+00
vc0734	*aceB*	Malate synthase A	2,24	1,4E-06
vc2507		PhoH family protein	2,23	0,0E+00
vc1344	*hppD*	4-hydroxyphenylpyruvate dioxygenase	2,22	6,9E-15
vca0219	*hlyA*	Hemolysin	2,20	5,7E-14
vca0159		putative Universal stress protein family 1	2,17	2,9E-15
vca0987	*ppsA*	phosphoenolpyruvate synthase	2,15	2,6E-09
vca0359	*parE2*	Plasmid stabilization system ParE protein (toxin of TA system ParD-ParE)	2,14	9,4E-10
vca0004		conserved hypothetical protein	2,14	0,0E+00
vc1222	*ihfA*	integration host factor subunit α	2,13	0,0E+00
vc2758	*fadB*	fatty acid oxidation complex subunit alpha FadB	2,10	6,1E-10
vc2704		conserved hypothetical protein	2,10	8,9E-09
vc1962	*nlpE*	copper resistance protein NlpE N-terminal domain-containing protein	2,08	3,9E-09
vca0278	*glyA*	serine hydroxymethyltransferase	2,04	0,0E+00
vca0280	*gcvT*	glycine cleavage system aminomethyltransferase	2,04	4,4E-16
vc0976	*qmcA*	putative Membrane protease subunits, stomatin/prohibitin homolog qmcA	2,03	6,5E-06
vc1539a		hypothetical protein	2,02	6,9E-10
vc0666		conserved hypothetical protein	2,02	1,8E-09
vc2144	*flaF*	Polar flagellin F	2,01	3,0E-13

DOWNREGULATED				
Locus	**Name**	**Annotation**	**Fold change Δ*vchM*/WT**	**p-value**
vca0198	*vchM*	Cytosine-specific DNA methyltransferase	-12,22	1,4E-24
vca0933	*cspE*	transcription antiterminator and regulator of RNA stability	-8,41	1,0E-07
vca0017	*hcp*	Haemolysin co-regulated protein (putative Type VI secretion system effector, Hcp1)	-3,20	1,3E-10
vc2383	*ilvY*	putative Transcriptional regulator, LysR family	-3,14	5,9E-27
vca0804	*deaD*	Cold-shock DEAD box protein A	-3,12	6,5E-49
vca0874		conserved hypothetical protein	-3,10	1,1E-05
vc1704	*metE*	5-methyltetrahydropteroyltriglutamate--homocysteine methyltransferase	-3,02	7,6E-21
vc0768	*guaA*	GMP synthetase	-2,91	2,7E-72
vca0680	*napC*	Cytochrome c-type protein napC	-2,87	2,4E-07
vca0679	*napB*	Diheme cytochrome c napB	-2,82	2,1E-06
vca0935		hypothetical protein	-2,76	1,2E-10
vc1261		putative Sugar efflux transporter B	-2,63	3,9E-07
vc0069	*mdtL*	putative FLORFENICOL EXPORTER	-2,53	8,1E-14
vca1002		AzlC family ABC transporter permease	-2,49	2,0E-08
vc1415	*hcp*	type VI secretion system secreted protein Hcp	-2,48	1,0E-06
vc0433	*arcD*	Arginine/ornithine antiporter	-2,48	1,9E-06
vc1393	*sugE*	Quaternary ammonium compound-resistance protein sugE	-2,43	3,4E-22
vc1035		conserved hypothetical protein	-2,40	6,3E-06
vc1608		ABC transporter permease	-2,38	2,8E-11
vca0250		Alpha-amylase	-2,37	7,2E-08
vc0767	*guaB*	inositol-5-monophosphate dehydrogenase	-2,31	3,0E-22
vc1239	*cobU*	cobinamide-P guanylyltransferase / cobinamide kinase	-2,28	1,2E-09
vc0290	*fis*	DNA-binding protein fis	-2,27	1,4E-04
vc2227	*purN*	phosphoribosylglycinamide formyltransferase 1	-2,25	2,6E-10
vc2384		TSUP family transporter	-2,24	8,1E-16
vca1003		AzlD domain-containing protein	-2,23	1,5E-11
vca0678	*napA*	Periplasmic nitrate reductase	-2,22	2,6E-10
vca1031		Methyl-accepting chemotaxis protein	-2,21	7,0E-11
vc1843	*cydB*	Cytochrome d ubiquinol oxidase subunit 2	-2,21	5,9E-13

vc0191	*rhtC*	putative Lysine/Homoserine/Threonine exporter protein	-2,20	2,6E-10
vc1609		ABC transporter permease	-2,19	2,2E-10
vc0005	*yidD*	membrane protein insertion efficiency factor	-2,16	4,9E-10
vc0291	*dusB*	tRNA-dihydrouridine synthase B	-2,16	3,8E-16
vc1855	*dinG*	ATP-dependent DNA helicase DinG	-2,15	7,7E-07
vc2382		conserved hypothetical protein	-2,15	3,1E-07
vc1842	*cydX*	cytochrome bd-I oxidase subunit CydX	-2,14	1,8E-06
vc1629		ABC transporter permease	-2,13	3,0E-06
vc0706	*raiA*	Ribosome-associated inhibitor A	-2,13	1,1E-08
vc2047		SDR family oxidoreductase	-2,11	3,4E-23
vc1174	*trpE*	Anthranilate synthase component 1	-2,09	9,9E-18
vc1240		histidine phosphatase family protein	-2,09	1,5E-06
vc0940		conserved hypothetical protein	-2,07	1,3E-07
vc1487		glutaredoxin family protein	-2,06	8,0E-06
vca0214	*emrD*	multidrug efflux pump EmrD	-2,05	6,0E-12
vca0269		aspartate aminotransferase family protein	-2,04	2,2E-13
vc2647	*aphA*	Transcriptional regulator PadR family	-2,04	9,6E-56
vc2226	*purM*	Phosphoribosylformylglycinamidine cyclo-ligase	-2,02	9,3E-10
vc0651		putative Peptidase U32	-2,02	2,4E-13
vc1630		putative SalX, ABC-type antimicrobial peptide transport system, ATPase component	-2,02	2,5E-19
vca0684		MFS transporter	-2,02	9,3E-14
vc0717	*yegQ*	tRNA 5-hydroxyuridine modification protein YegQ	-2,01	4,2E-09
vc1856		TSUP family transporter	-2,00	7,2E-10
vc0987	*hemH*	ferrochelatase	-2,00	1,9E-17

Table S2. Strains, plasmids and primers used in this study

Strain	Lab Strain number	Source/Construction
Vibrio cholerae		

N16961 hapR+ WT strain	F606	Gift from Melanie Blokesch
Δ*vchM* (vca0198)	H507	PCR amplification of 500bp up and down genomic regions of VCA0198 using primers ZIP136/137 and ZIP138/139. PCR amplification of aadA7 conferring spectinomycin resistance on pAM34 using ZB47/48. PCR assembly of the VCA0198::spec fragment using ZIP136/139 and allelic exchange by natural transformation in F606.
Δ*lacZ*	K329	Lab collection
Δ*groESL-2* (*vca0819-0820*)	M958	allelic exchange by integration and excision of conjugative suicide plasmid pMP7 (pM340) replacing the gene with frt::kan::frt
Δ*vchM* Δ*groESL-2*	N330	PCR amplification of 500bp up and down genomic regions of VCA0198 using primers ZIP136/137 and ZIP138/139. PCR amplification of aadA7 conferring spectinomycin resistance on pAM34 using ZB47/48. PCR assembly of the VCA0198::spec fragment using ZIP136/139 and allelic exchange by natural transformation in M958
WT – VchM site #1 mutated (mut #1)	L900	allelic exchange by integration and excision of conjugative suicide plasmid pMP7 (pL442)
WT – VchM sites #1-4 mutated (mut #1-4)	Q827	allelic exchange by integration and excision of conjugative suicide plasmid pMP7 containing the *groESL-2* region with sites #1-4 mutated (pQ824) in M958 strain.
Δ*vchM* mut #1-4	Q828	allelic exchange by integration and excision of conjugative suicide plasmid pMP7 containing the *groESL-2* region with sites #1-4 mutated (pQ824) in N330
Plasmids		
pMP7-Δ*vca0819-0820*::kan	M340	gibson assembly using primers MV450/451 for the amplification of pMP7 vector, primers “vca0819-8205” and “vca0819-8206” for up and down regions of the gene, and primers MV268/269 on pKD4 plasmid for the resistance gene (frt::kan::frt).
pMP7- C->T point mutation	L442	Amplification of 500bp upstream of *vca0819* with primers 5923/5922; Amplification of 500bp downstream of *vca0819* with 5924/5921; PCR assembly of the two fragments with

of VchM site #1 in 5' UTR region of vca0819-0820		primers 5923/5924. Note: Primers 5922 and 5921 contain a mismatch to give origin to a C->T point mutation in VchM site #1. The fragment was then cloned in a pTOPO vector and sub cloned into pMP7 using *EcoRI* restriction sites.
pMP7- sites #1-4 mutated in vca0819-0820 region	Q824	A *groESL-2* fragment with mutations in VchM sites #2-4 was synthesized and cloned in a pTOPO vector. This fragment was then PCR assembled to the 5' UTR region containing site #1 mutated (from strain L900), which originated a final fragment containing the #1-4 mutated sites. This fragment was then cloned in pTOPO and sub cloned into pMP7 using *EcoRI* restriction sites.
pSC101-*groESL-1*	O849	Amplification of *vc2664-2665* from *V. cholerae* gDNA with primers AFC046/AFC047. Primer AFC046 contains a Ptrc promoter. Fragment cloned in pSC101 low copy plasmid (carbenicillin resistant) using *EcoRI* restriction sites
pSC101-*groESL-2*	N752	Amplification of *vca0819-0820* from *V. cholerae* gDNA with primers AFC029/AFC030. Primer AFC029 contains a Ptrc promoter. Fragment cloned in pSC101 low copy plasmid (carbenicillin resistant) using *EcoRI* restriction sites
pSC101-*vchM*	Q826	Amplification of *vca0198 (vchM)* with its own promoter from *V. cholerae* gDNA with primers 5990/5911. Cloning in pTOPO vector and sub cloning in pSC101 low copy plasmid (carbenicillin resistant) using *BamHI* and *PstI* restriction sites
Primers		**Sequence 5'-3'**
ZIP136		GCCGCCGAAGGAAAAACCGTACTATTGC
ZIP137		GCGAGCATCGTTTGTTCGCCCAGCTTCTGTATGGAACGGGTTAACT GTATCACCATACTACCTCATGG
ZIP138		CGTGAAAGGCGAGATCACCAAGGTAGTCGGCAAATAATGTCTACA TGCTTCACAGCGTAGTCGC
ZIP139		TTAATTTCTCGAGTTTCAGATGC
ZB47		CCCGTTCCATACAGAAGCTGGGCGAACAAACGATGCTCGC
ZB48		GACATTATTTGCCGACTACCTTGGTGATCTCGCCTTTCACG
vca0819-8205		CTATTATTTAAACTCTTTCCGTTTTGCCTT
vca0819-8206		TACGTAGAATGTATCAGACTCGCCCAAGGA
5921		AAACAATCCTA**T**CGGCCTTTTATC
5922		GATAAAAGGCCG**A**TAGGATTGTTT

5923		ACTTTGATGGTACGCGCGATG
5924		GATTTATTGAGCACAACATGGCG
AFC029		GTAAGTGAATTCTTGACAATTAATCATCCGGCTCGTATAATGTGTG GAATTGTGAGCGGATAACAATTTCACACAGGAAACAGCGCCGCAT GAATATTCGTCCTTTACATG
AFC030		GTAAGTGAATTCATTACGCCGCAGACTCTTTGTC
AFC046		GTAAGTGAATTCTTGACAATTAATCATCCGGCTCGTATAATGTGTG GAATTGTGAGCGGATAACAATTTCACACAGGAAACAGCGCCGCAT GAATATTCGTCCATTACATGAC
AFC047		GTAAGTGAATTCCTGCTAAGGGGGATGATTACA
5990		GTTTTTGCTGCCGTCTGCTA
5911		GTAGTCGACCCTTTTTACAAACTTTCTAGA

826

827

828 **Table S3. Primer and probe sequences used in digital qRT-PCR**

Target	Primers (5'-3')	Probes (5'-3')
gyrA	AATGTGCTGGGCAACGACTG	[Cy5]-CACCCTCATGGTGACAGTGCGGTTT-[BHQ2]
	GAGCCAAAGTTACCTTGGCC	
groES-1	CGTAGCTTTCTGCGAAGATC	[HEX] -AGCTCCAAAGGTTGAACTGAACCGTTCTCTA-[BHQ1]
	TGGTGGAATTGTTCTAACTG	
groES-2	GGCGACCAGATCATTTTCAAC	[FAM] - TGGACGGTAAAGAGTATCTGATCCTCTCC-[BHQ1]
	TCTACAATCGCTAACACATCAG	
groEL-2	TGCTATCGTTCAGAATCAACC	[HEX] –AAGCTTACCAGCATAGAACTTGCCAGAGAT-[BHQ1]
	TTTACTTCTCGCTCCCAATCG	

829

830

831

832

833

834

835

836

837

838 **S1 Figure**

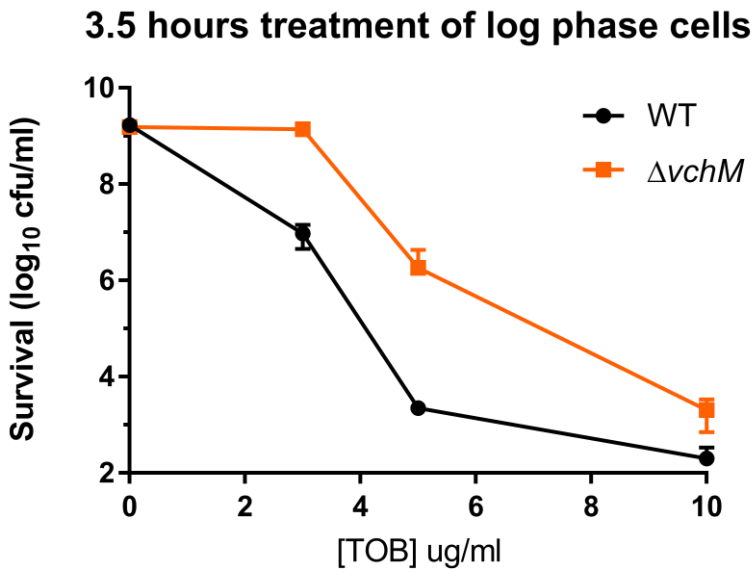

839

840

841 **S2 Figure**

842

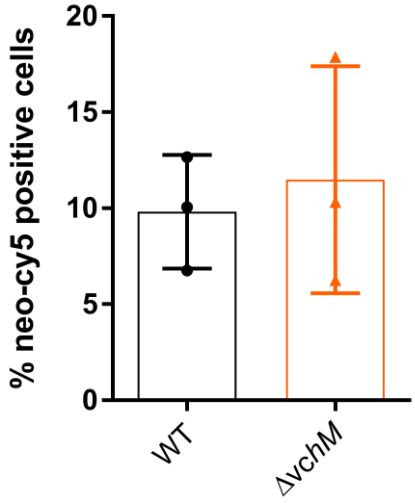

843

844

845

S3 Figure

	Eco GroES	*Vch* GroES-1	*Vch* GroES-2
Eco GroES (97aa)		80.21	65.62
Vch GroES-1 (96aa)	80.21		65.62
Vch GroES-2 (96aa)	65.62	65.62	

	Eco GroEL	*Vch* GroEL-1	*Vch* GroEL-2
Eco GroEL (541aa)		86.77	74.34
Vch GroEL-1 (544aa)	86.77		76.18
Vch GroEL-2 (530aa)	74.34	76.18	

S4 Figure

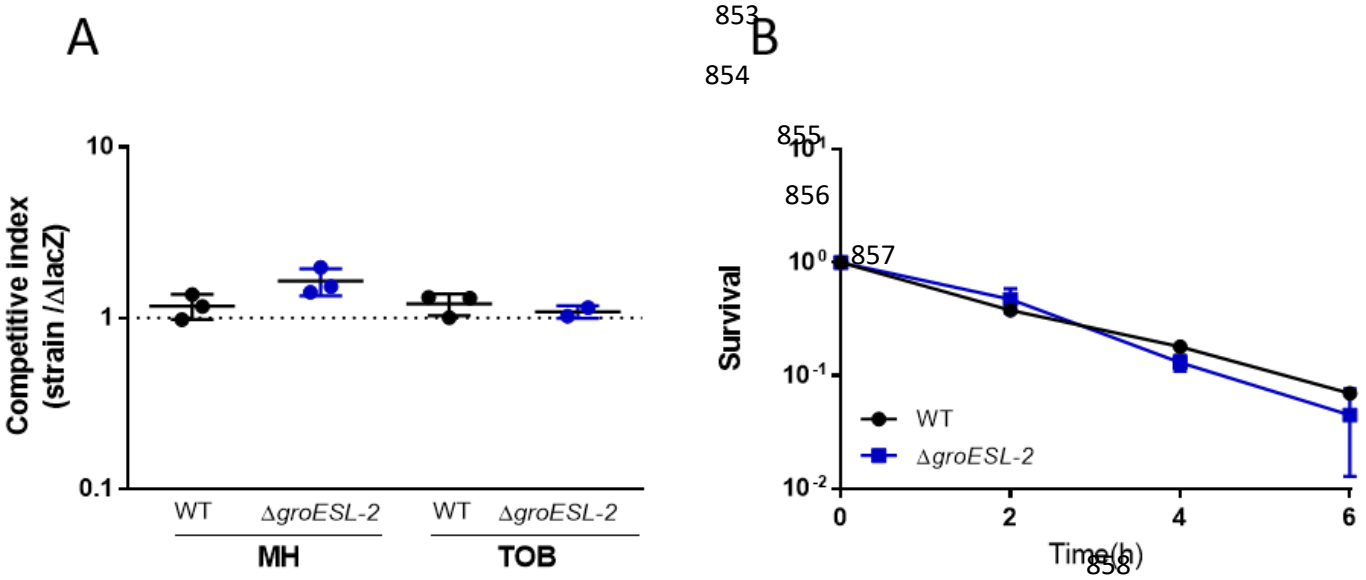

862

863 **S5 Figure**

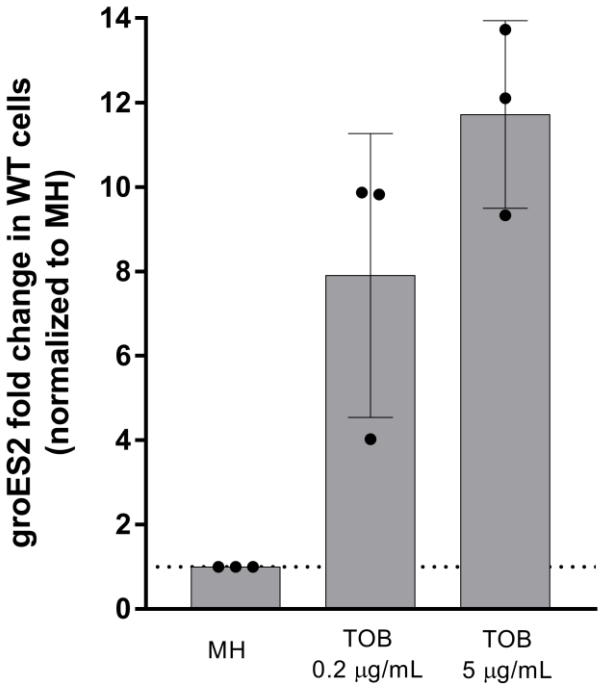

864

865

866 **S6 Figure**

867

868

869

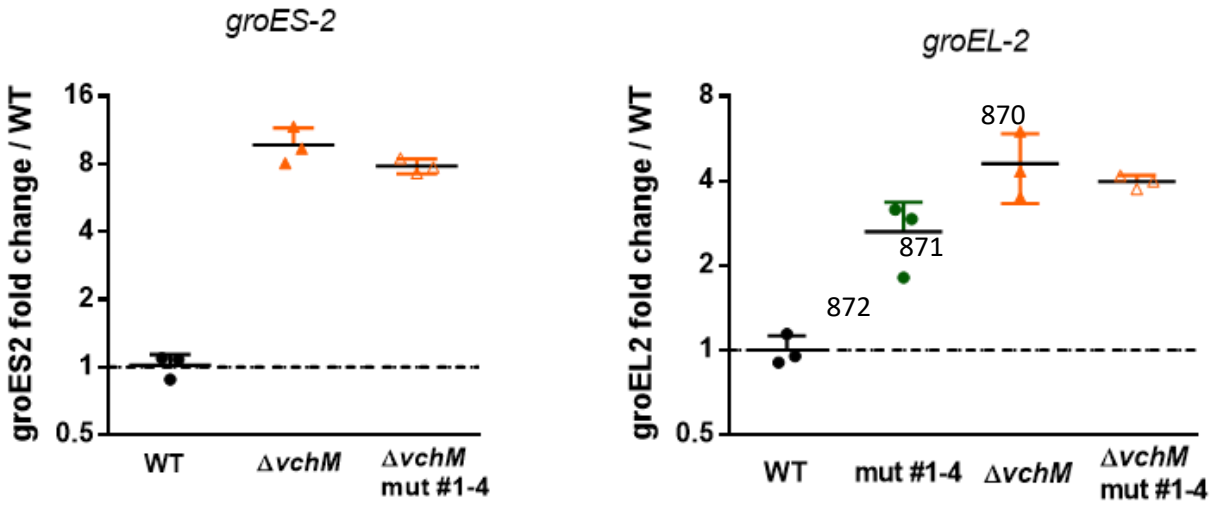

873

874

S7 Figure